Tunable atom-light beam splitter using electromagnetically induced transparency

Xinyu Zhu, Rong Wen, and J. F. Chen*
Quantum Institute of Light and Atoms, Department of Physics, School of Physics and Materials Science, East China Normal University, Shanghai 200241, People's Republic of China

(Received 5 January 2018; published 1 June 2018)

With electromagnetically induced transmission (EIT), an optical field can be converted into collective atomic excitation and stored in the atomic medium through switching off the strong-coupling field adiabatically. By varying the power of the coupling pulse, we can control the ratio between the transmitted optical field and the stored atomic mode. We use a cloud of cold ^{85}Rb atoms prepared in magneto-optical trap as the experimental platform. Based on a model of EIT dark-state polariton, we consider the real case where the atomic medium has a finite length. The theoretical calculation gives numerical results that agree well with the experimental data. The results show that the ratio can be changed approximately from 0 to 100%, when the maximum power of the coupling pulse (the pulse length is 100 ns) varies from 0 to 20 mW, in the cold atomic ensemble with an optical depth of 40. This process can be used to achieve an atom-light hybrid beam splitter with tunable splitting ratio and thus find potential application in interferometric measurement and quantum information processing.

DOI: 10.1103/PhysRevA.97.063801

I. INTRODUCTION

Beam splitters are linear devices widely used in quantum information processing. In a typical beam-splitter model, the mixing waves are of the same type, for example, optical waves [1–4] or atomic waves [5–7]. Recent works report the splitting and mixing of waves between different types, i.e., optical waves and atomic spin waves, through Raman scattering [8,9] or photon echo [10]. The atomic spin wave, which is the collective atomic excitation introduced by Raymer *et al.* [11], can be used to store optical qubits and be retrieved in an optical wave when desired [12–14]. Therefore, the atomic ensemble driven by an external optical field is considered as a atom-light hybrid beam splitter [8,9], which operates between the optical mode and the atomic excitation. With the coherent interference between atoms and light in such hybrid beam splitters, one arm of the interferometer is stored as the atomic coherence in the atomic medium.

Apart from the Raman process, electromagnetically induced transparency (EIT) [15] coherently produces atomic spin waves when a weak optical field is injected. With the strong-coupling field slowly varying, a reversible transformation between the optical field and the atomic spin wave occurs, with their composite, termed a dark-state polariton, conserved [16,17]. Electromagnetically induced transparency is widely used to demonstrate quantum optical memory [13,18–22] and more than 90% of the storage efficiency [23] is realized with the medium, probe, and coupling field appropriately prepared.

As is well known in the model of the EIT dark-state polariton [16], the mixing angle $\theta(z,t)$ is introduced as a parameter for the ratio between the optical field $\hat{E}$ and the collective atomic excitation $\hat{S}$. Assuming the coupling field Ω_c is changing adiabatically, a quantum field $\Psi_D(z,t)$ representing the quasiparticles dark-state polaritons can be introduced,

$$\Psi_D(z,t) = \cos\theta(z,t)\hat{E}(z,t) - \sin\theta(z,t)\hat{S}(z,t). \quad (1)$$

The mixing angle $\theta(z,t)$ is given as $\tan^2\theta(z,t) = g^2 N_z/\Omega_c^2(t)$, where g is the atom-light coupling coefficient and N_z is the number of atoms in a thin slice at location z. Reversible transfer occurs between the optical field and the atomic coherence with a slowly varying coupling field $\Omega_c(t)$. In the application of optical quantum memory, through adiabatically changing the coupling field to tune θ from 0 to $\pi/2$, an optical field can be fully stored in the atoms and vice versa. However, $\cos\theta$ and $\sin\theta$ cannot be simply considered as the splitting coefficients for the optical mode and the collective atomic mode because Eq. (1) is obtained from the model where the optical pulse propagates in an infinitely long medium. Actually, the standard experimental parameters give $g^2 N_z \gg \Omega_c^2$. Without considering the boundary of the finite-size medium where N_z decrease to zero, $\sin\theta$ is always close to 1. A theoretical model is lacking which considers the splitting ratio between the transmitted optical field and the collective atomic mode, provided a coupling pulse is applied to the atomic cloud with finite length.

In this paper, via changing the power of the coupling pulse, we change the splitting ratio between the optical wave and atomic spin wave through a cold atomic cloud with an EIT process. Experimentally, with the appropriate design of the probe and coupling pulse, the splitting ratio of this atom-light hybrid beam splitter can be manipulated with equal portions. Theoretically, we calculate the splitting ratio based on the model of the EIT dark-state polariton [16], but within an atomic medium of finite length. The numerical calculation gives results which agree well with the experimental data and the simulation given by the evolution equations of the atomic operators in the Heisenberg picture and the propagation of an optical wave governed by the Maxwell equation. It

*jfchen@phy.ecnu.edu.cn

indicates that our simplified model works well for calculating the splitting ratio of the dark-state polaritons.

II. THEORETICAL MODEL

We consider an atomic cloud consisting of a total of N atoms and N_z atoms in a thin slice at position z ($N \gg N_z \gg 1$), with Λ-type three-level atomic energy levels, i.e., the ground state $|1\rangle$, a metastable state $|2\rangle$, and an excited state $|3\rangle$. The collective atomic operator is defined as $\hat{\sigma}_{\mu\nu}(z,t) = \frac{1}{N_z}\sum_{i=1}^{N_z} |\mu_i\rangle\langle\nu_i| e^{-i\omega_{\mu\nu}t}$, where $\mu, \nu = 1,2,3$. The dephasing rates are given by $\gamma_{13} = \gamma_{23} = 2\pi \times 3$ MHz and $\gamma_{12} = 0.01\gamma_{13}$. A time-varying optical field $\Omega_c(t)$ resonantly couples the states $|2\rangle$ and $|3\rangle$ and a weak optical field $\hat{E}(z,t)$ with photons n ($n \ll N_z$) through the transition $|1\rangle \rightarrow |3\rangle$. The optical field operator obeys the Maxwell wave equation

$$\left(\frac{\partial}{\partial t} + c\frac{\partial}{\partial z}\right)\hat{E}(z,t) = igN_z\hat{\sigma}_{13}. \tag{2}$$

Here $g = \mu\sqrt{\omega_p/2\hbar\varepsilon_0 V}$ is the atom-light coupling constant, where μ denotes the dipole moment, ω_p denotes the carrier frequency of the optical field, and V is the quantization volume containing N_z atoms. For simplicity, we assume that N_z/V is a constant value through the atomic medium and equal to the atomic density N_d averaged over the whole volume of the medium. The evolution of the atomic operators in the Heisenberg picture is described by the equations

$$\dot{\hat{\sigma}}_{11} = -\frac{i}{2}g\hat{E}(z,t)\hat{\sigma}_{13} + \frac{i}{2}\hat{\sigma}_{31}g\hat{E}(z,t) + 2\gamma_{13}\hat{\sigma}_{33}, \tag{3}$$

$$\dot{\hat{\sigma}}_{13} = -\gamma_{13}\hat{\sigma}_{13} - \frac{i}{2}\Omega_c(t)\hat{\sigma}_{12} + \frac{i}{2}g\hat{E}(z,t)(\hat{\sigma}_{33} - \hat{\sigma}_{11}), \tag{4}$$

$$\dot{\hat{\sigma}}_{12} = -\gamma_{12}\hat{\sigma}_{12} + \frac{i}{2}g\hat{E}(z,t)\hat{\sigma}_{32} - \frac{i}{2}\Omega_c(t)\hat{\sigma}_{13}, \tag{5}$$

$$\dot{\hat{\sigma}}_{22} = -\frac{i}{2}\Omega_c(t)\hat{\sigma}_{23} + \frac{i}{2}\hat{\sigma}_{32}\Omega_c^*(t) + 2\gamma_{23}\hat{\sigma}_{33}, \tag{6}$$

$$\dot{\hat{\sigma}}_{23} = -\gamma_{23}\hat{\sigma}_{23} + \frac{i}{2}\Omega_c^*(t)(\hat{\sigma}_{33} - \hat{\sigma}_{22}) - \frac{i}{2}g\hat{E}(z,t)\hat{\sigma}_{21}, \tag{7}$$

$$\hat{\sigma}_{33} = 1 - \hat{\sigma}_{22} - \hat{\sigma}_{11}. \tag{8}$$

The evolution equations for the atomic operators and the optical field in the Heisenberg picture provide numerical simulation results for the optical field and retrieved atomic coherence from the atomic cloud, with $\Omega_c(t)$ designed. This universal approach, without providing any physical picture, gives numerical results for the propagation of the optical pulse and collective atomic coherence.

If $\Omega_c(t)$ is changing sufficiently slowly, in the adiabatic limit, Eqs. (2)–(8) can be simplified as the propagation of a new quantum field called a dark-state polariton Ψ_D. In this model of the dark-state polariton, the collective atomic mode is directly related to the collective atomic operator $\hat{\sigma}_{12}(z,t) = \frac{1}{N_z}\sum_{i=1}^{N_z} |1_i\rangle\langle 2_i| e^{-i\omega_{12}t}$: $\hat{S}(z,t) = \sqrt{N_z}\hat{\sigma}_{12}(z,t)$. The atom-light beam splitter is formed by four ports, which can be modeled similarly to a standard beam splitter as shown in Fig. 1. One important difference is that the input and output ports of the collective atomic modes $\hat{S}$ are both located inside the atomic medium and thus cannot spatially separate as a normal spatial splitter. Furthermore, the splitting process is driven by an external coupling pulse and therefore we consider the splitting behavior over an accumulated time. The effective Hamiltonian for generating the atomic excitation $\hat{\sigma}_{12}$ with a probe annihilation operator $\hat{E}$ and a strong coupling field Ω_c can be expressed as

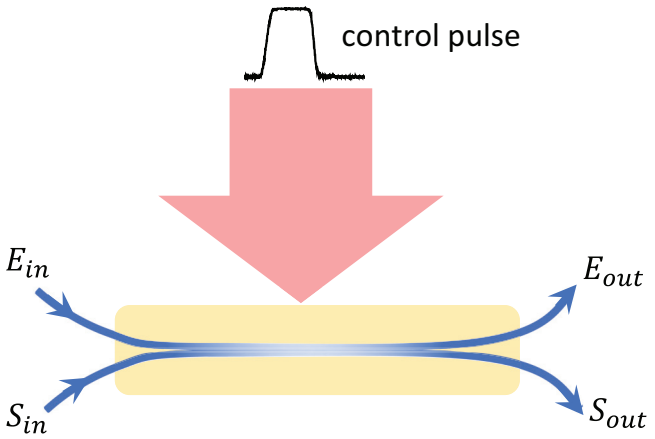

FIG. 1. Input and output ports of the atom-light beam splitter. A control (coupling) pulse is applied to the medium to induce the atom-light interaction for the transformation.

$$H_{\text{eff}} = \sum_j g\hat{E}e^{ikz}\sigma_{12,j}^{\dagger}\Omega_c^{\star}e^{-ik_c z + i\phi} + \text{H.c.}, \tag{9}$$

in which the atomic operator $\hat{\sigma}_{12}$ is summed over j atoms. Here k and k_c are the wave vectors of the probe and coupling beam, respectively, projected on the z axis, and we consider the simplest case in a cold atomic cloud, $k \approx k_c$. In addition, ϕ is the relative phase of the coupling field with respect to the probe field and is well controlled in experiments. From Eq. (9), the collective atomic mode obtains a phase as $\hat{S} = \sqrt{N_z}\hat{\sigma}_{12}e^{-i\phi}$. Conversely, to retrieve the atomic excitation in an optical field, a second coupling field (with Ω_c and k_c') is applied. The effective Hamiltonian can be expressed as

$$H'_{\text{eff}} = \sum_j g\hat{E}^{\dagger}e^{-ikz}\sigma_{12,j}e^{-i\phi}\Omega_c e^{ik_c' z - i\phi'} + \text{H.c.} \tag{10}$$

If the second coupling field also has a well-defined phase ϕ' relative to the first coupling field, the retrieved optical pulse has a definite phase relation with the input optical field. The magnitude of the splitting coefficients of the transmitted optical field and the collective atomic mode is tunable. In the following, we denote them by $|u|^2$ and $|v|^2$, respectively. Interferometry utilizing these two fields can be done by resending the escaping optical pulse back into the atomic ensemble, and after a second coupling pulse, the atomic excitation can be retrieved in an optical field which interferes with the return optical pulse. In this work, we theoretically and experimentally demonstrate that $|u|^2$ and $|v|^2$ depend on the power of the control pulse. These two magnitudes can be easily measured in experiments by measuring the transmitted signal pulse and the retrieved pulse from another reading pulse. The physical model discussed below, for simplicity, considers no absorption occurring in the atomic medium. The energy of the transmitted optical field and the stored atomic coherence is equal to the

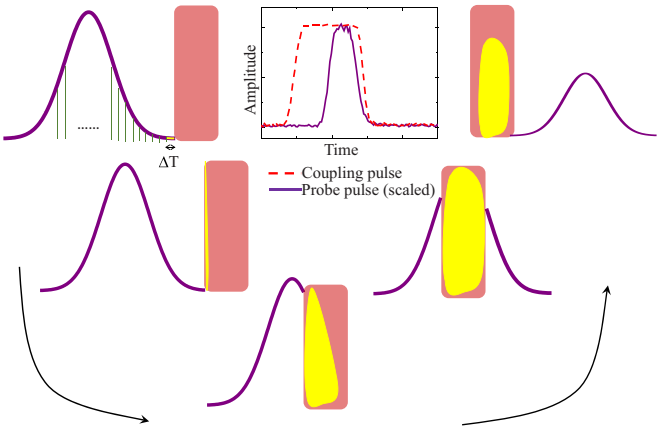

FIG. 2. Propagation of an optical pulse through a cold atomic cloud with finite length L. The envelope of the optical pulse is $f(T)$ and is divided into many slices of ΔT in the dark-state polariton model. Every slice enters the medium and propagates with the slow group velocity V_g, which is dependent on the time-varying coupling field Ω_c. When the slices propagate to the output side of the medium, i.e., $z = L$ where $N_z \to 0$, they exit the medium as the transmitted optical wave.

energy of the input optical field, i.e., $|u|^2 + |v|^2 = 1$. However, absorption in this atom-light beam splitter is inevitable in experiments. The first reason is the nonzero dephasing rate γ_{12}, which gives rise to nonunity transmission at the center of the EIT transparency window. Another cause of absorption is the mismatch between the input optical pulse and the EIT transmission window in the spectrum. Luckily, we are able to measure the absorption coefficient A, as described in the following section. The absorption A can be taken into account when we normalize $|u|^2 + |v|^2$ to $1 - A$.

To properly evaluate the splitting ratio of the atom-light beam splitter, we consider the whole pulse propagation process in the atomic cloud with finite size L. Here, in the model described below, we ignore the absorption of the atomic cloud. As shown in Fig. 2, the optical field $\hat{E}$ is applied to the atomic medium via a probe pulse, which starts after the coupling field is established and ends before the coupling field is fully switched off. Before entering the medium at $z = 0$, the optical field propagates with the speed of vacuum c and behave as a pulse train with spatial length much longer than the medium. After entering the atomic medium, the dark-state polariton, which is composed of an optical field $\hat{E}$ and a collective atomic mode $\hat{S}$, propagates with the group velocity $V_g = c\cos^2\theta$. The wave front of the probe pulse will enter the medium first and propagates in the medium as an optical field $\hat{E}$ when the amplitude of the coupling field is constant in time at the very beginning. With the coupling field slowly switching off, i.e., $\partial\Omega_c/\partial t \neq 0$, reversible changes between the optical field and the atomic excitation occur. Since in the usual case $g^2 N_z \gg \Omega_c$, the optical field is transferred to the atomic excitation whenever it enters the medium. On the other hand, with a reducing Ω_c, the new quantum field in the medium propagates slower with a continuously decreasing V_g and finally stops in the medium when the coupling field is fully switched off. However, before the coupling field is fully off, the wave front of the quantum field, which enters the medium at a very early time, can escape to the boundary of the medium where $N_z \to 0$. In consequence, some part of the incident optical field is transferred into the collective atomic excitation and some propagates throughout the medium as the transmitted pulse. In this way, the medium which is driven by an external pulse can be considered as a beam splitter for splitting energy between the optical field and the atomic excitation.

According to this model, we therefore divide the incident optical pulse into many slices ΔT, as shown in Fig. 2. Each slice of ΔT enters the medium one by one and they do not overlap with each other in space. This is a reasonable assumption, since the group velocity is continuously reducing and the latter slice will not surpass the former. For each slice, considering Ω is changing adiabatically and thus for each small time interval the group velocity is a constant, we evaluate its travel distance in the medium before the coupling field is switched off. If the travel distance is larger than the effective length of the atomic cloud L, the slice contributes to the final transmitted pulse, i.e., $\Sigma_{\Delta T\to 0}\Delta T\langle\hat{E}^\dagger(L,T)\hat{E}(L,T)\rangle$. Otherwise, the slice contributes to the atomic excitation.

III. EXPERIMENTAL RESULTS AND DISCUSSION

The medium is composed of ^{85}Rb atoms in a two-dimensional magneto-optical trap (MOT) with length $L = 1.5$ cm and diameter about 1 mm [24]. The system is run periodically with a MOT preparation time of 4.5 ms followed with a measurement window of 0.5 ms. The center gradient of the two-dimensional MOT quadrature magnetic field is 10 G/cm and always remains on. The atomic optical depth is 40 and the atomic density N_d of cold atoms is about 4×10^{10} cm^{-3}. Figure 3(a) shows the energy-level diagram of the three-level Λ system, where $|1\rangle = |5S_{1/2}, F = 2\rangle$, $|2\rangle = |5S_{1/2}, F = 3\rangle$, and $|3\rangle = |5P_{1/2}, F = 3\rangle$. The atomic decay rate of the excited state $|3\rangle$ is $\Gamma_3 = 2\pi \times 6$ MHz. The dephasing rates $\gamma_{13} = \gamma_{23} = (1/2)\Gamma_3$ and $\gamma_{12} \approx 0.01\gamma_{13}$. Initially 98% of the atoms are prepared in the ground state $|1\rangle$. Figure 3(c) shows the experimental setup for the measurement. The input optical field is injected into the atomic cloud through the probe laser. The probe and coupling beams, originated from the same diode laser, are respectively frequency shifted using acousto-optics modulators and therefore the two-photon detuning is well controlled to be zero. As shown in Fig. 3(a), the probe beam is on resonance with the atomic transition $|1\rangle \to |3\rangle$ and the coupling beam is on resonance with $|2\rangle \to |3\rangle$. The weak (100 nW) probe laser beam is aligned with the longitudinal axis of the atomic cloud and is focused with a $1/e^2$ diameter of 230 μm at the region of the trapped atomic cloud. The transmitted $\hat{E}$ is collected by a photomultiplier tube (PMT). To enable the slowly changing coupling field covering the whole atomic cloud, the coupling laser beam is a collimated beam with a $1/e^2$ diameter of 1.6 mm. Also, the coupling beam deviates from the longitudinal axis by 2.5°, to minimize the scattered noise into the PMT. Also, to take advantage of the most Zeeman sublevels for EIT channels, the polarization of the probe and coupling beams is σ^+ (or σ^-).

Figure 3(b) shows the timing sequence of coupling and probe pulses. The falling edge of the first coupling pulse, whose full width at half maximum (FWHM) is 100 ns, overlaps with the probe pulse (with a FWHM of 50 ns). Therefore, the $\hat{E}$

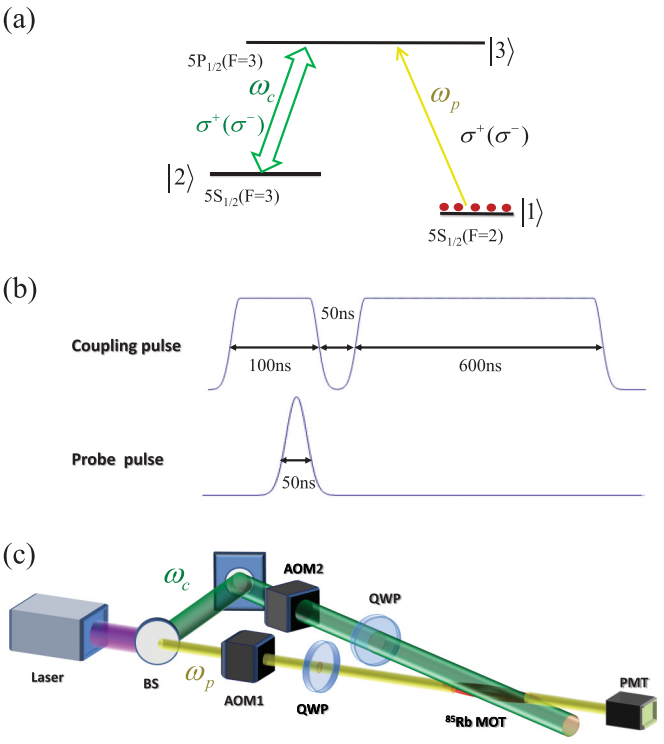

FIG. 3. Experimental schemes: (a) the Λ-type three-level system used for the atom-light beam splitter, (b) the timing of the experiment, and (c) an experimental sketch of the atom-light beam splitter. The coupling beam and the probe beam are circularly polarized and originate from the same diode laser. The coupling beam deviates from the longitudinal axis of the cloud by 2.5° and effectively covers the whole atomic cloud. Here BS denotes beam splitter, AOM acousto-optic modulator, and QWP quarter-wave plate.

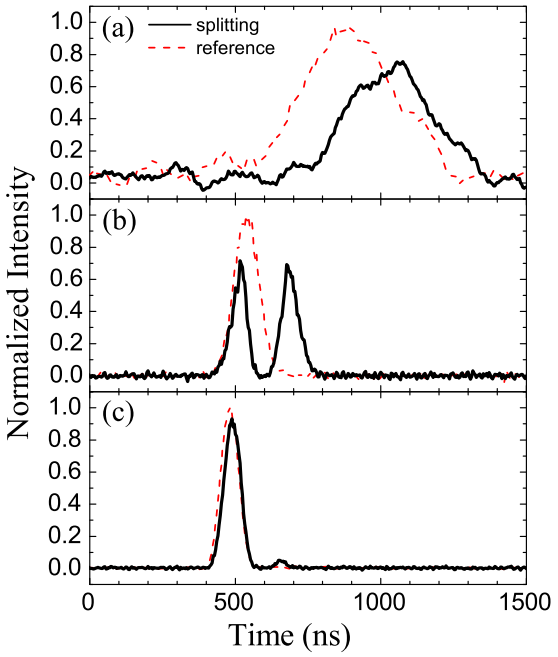

FIG. 4. Normalized intensity detected by the PMT with different power for the coupling pulse. The red dashed lines represent the reference, which is measured with a continuous coupling field operating on the atomic cloud. This reference is used to calculate the splitting coefficients $|u|^2$ and $|v|^2$ below. The black solid lines represent the signal measured in the hybrid splitter with coupling powers of (a) 0.5 mW, (b) 3 mW, and (c) 12.5 mW.

can be transferred into the collective atomic mode $\hat{S}$ with a decreasing coupling field Ω_c. After 50 ns of delay, which is still in the lifetime of the atomic spin excitation, a second coupling pulse is to retrieve the atomic spin excitation to be an optical field for measurement. To make sure the stored atomic spin excitation is retrieved by almost 100%, the second coupling is extended to 600 ns, which is equivalent to multiple sequences of short retrieval pulses [25] at high retrieving beam power. Therefore, the first coupling pulse serves as the driving field for the atom-light beam splitter, where part of the optical field is transferred into the atomic spin excitation, and the second one serves as the retrieving pulse for measuring the atomic excitation. As described in the above theoretical model, changing Ω_c can efficiently change the splitting ratio for the hybrid beam splitter.

The transmitted $\hat{E}$ and the retrieved $\hat{S}$ are depicted in Fig. 4, with the coupling Rabi frequency Ω_c as $3.08\gamma_{13}$, $7.53\gamma_{13}$, and $15.38\gamma_{13}$, respectively. When the coupling field is switched on and off as the timing sequence described above, the reversible changes between the light and atomic spin occur. The dark solid lines denote the transmitted $\hat{E}$ field followed by the atomic spin retrieved by the second coupling pulse. With a small coupling field Ω_c [Fig. 4(a)], the transmitted optical field is trivial and not recognizable because most of the input optical field is transformed as the atomic spin excitation. Also, due to the slow group velocity $v_g = c\cos^2\theta$, the retrieved pulse is deformed and delayed severely, as shown in Fig. 4(a). With a larger Ω_c, Fig. 4(b) shows a ratio of 50:50. When $\Omega_c = 15.38\gamma_{13}$, over 95% of the input field is transmitted through the medium and therefore the retrieved atomic spin excitation is negligible, as shown in Fig. 4(c).

As discussed in the above theoretical model, the absorption A in the medium cannot be ignored. Furthermore, A differs with the changing value of Ω_c. In experiment, we have the coupling beam continuously on and thus the input optical pulse will be maintained as the optical mode without being transferred into atomic modes. The transmitted pulse is thus measured through the same PMT, as shown by the red dashed lines in Fig. 4, with pulse area equal to $1 - A$. Therefore, with this transmitted pulse as a reference, we normalize the splitting ratio as $|u|^2 = \mathcal{A}_E/\mathcal{A}_{\rm ref}$ and $|v|^2 = \mathcal{A}_S/\mathcal{A}_{\rm ref}$ (where $\mathcal{A}$ denotes area) and $|u|^2 + |v|^2 = 1$ is still applicable.

While changing the coupling Ω_c, we are able to tune the splitting ratio ($|u|^2$ or $|v|^2$) from 0 to 100%. The tunable splitting ratio is shown in Fig. 5, where $|u|^2$ ($|v|^2$) is calculated from the ratio of the transmitted (retrieved) pulse area to the reference pulse area. The squares and circles with error bar represent the experimental data. We plot the numerical curves obtained according to the dark-state polariton (DSP) model described above and the simulation results according to the Maxwell-Heisenberg evolution equations (2)–(8). From Fig. 5 the experimental data match the DSP model well, except the splitting ratio $|v|^2$ for the low-Ω_c case. In this

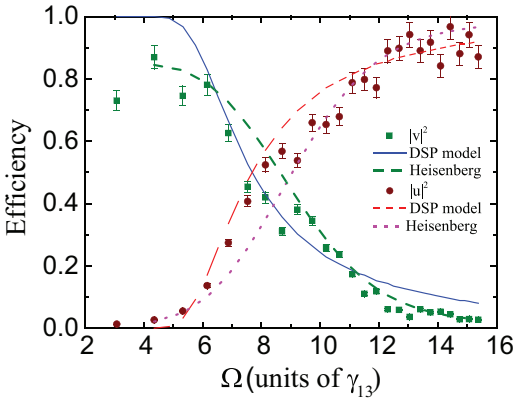

FIG. 5. Tunable splitting ratio. The red dashed line represents $|u|^2$ obtained from the DSP model and the blue solid line is for $|v|^2$. The crimson circles and green squares with error bars are the experimental data. The purple dotted line and the green short-dashed line show the numerical results from the Maxwell-Heisenberg equations. The pulse envelopes of the coupling field and the input weak optical field are designed as shown in Fig. 3(b).

regime, due to the nonzero dephasing rate γ_{12}, the EIT loss term $1-\exp(-4OD\gamma_{12}\gamma_{13}/|\Omega_c|^2)$ increases severely when Ω_c decreases. Hence the absorption of the medium is not a constant in this regime. Also from Fig. 5 it is clear that the 50:50 splitting ratio occurs at $\Omega_c = 7.5\gamma_{13}$, which corresponds to the cw coupling power of 2.9 mW in our system. Compared to the universal Maxwell-Heisenberg equations, the DSP model correctly predicts the 50:50 splitting point. The working point of the 50:50 splitting ratio will be useful for operation of the atom-light interferometer.

IV. CONCLUSION

Through controlling the power of the coupling pulse, we vary the splitting ratio from 0 to 100% between the optical field and the collective atomic mode generated from the EIT process. The process is equivalent to a tunable beam splitter. According to the EIT dark-state polariton model, we evaluate the propagation of the incident optical field in the atomic medium with finite size and simulate the splitting ratio after considering the boundary effect of the medium. We verify that the experimental curves agree well with our theoretical calculation. One possible application of the tunable beam splitter is to establish an atom-light interferometer for phase measurement. Similar to the schematic setup in Refs. [8,9], the transmitted optical pulse can be sent out and redirected into the atomic cloud via the Sagnac interferometric scheme. The phase modulation can be added through the traveling optical pulse or through the collective atomic mode $\hat{S}$ by changing the surrounding magnetic or electric field. Another further application lies in the situation of weak signal input, e.g., a single-photon source. This is to generate an entangled state of photons with different color for quantum information processing, i.e., a visible optical mode and an atomic spin mode in the microwave regime.

ACKNOWLEDGMENTS

This work was supported by the National Key Research and Development Program of China under Grant No. 2016YFA0302001, the National Natural Science Foundation of China through Grants No. 11674100 and No. 11654005, the Natural Science Foundation of Shanghai through Grant No. 16ZR1448200, and the Shanghai Rising-Star Program No. 17QA1401300.

[1] M. Zukowski, A. Zeilinger, M. A. Horne, and A. K. Ekert, Phys. Rev. Lett. **71**, 4287 (1993).
[2] P. Walther, J.-W. Pan, M. Aspelmeyer, R. Ursin, S. Gasparoni, and A. Zeilinger, Nature (London) **429**, 158 (2004).
[3] R. Kaltenbaek, B. Blauensteiner, M. Zukowski, M. Aspelmeyer, and A. Zeilinger, Phys. Rev. Lett. **96**, 240502 (2006).
[4] T. Legero, T. Wilk, M. Hennrich, G. Rempe, and A. Kuhn, Phys. Rev. Lett. **93**, 070503 (2004).
[5] T. L. Gustavson, P. Bouyer, and M. A. Kasevich, Phys. Rev. Lett. **78**, 2046 (1997).
[6] A. Lenef, T. D. Hammond, E. T. Smith, M. S. Chapman, R. A. Rubenstein, and D. E. Pritchard, Phys. Rev. Lett. **78**, 760 (1997).
[7] R. Lopes, A. Imanaliev, A. Aspect, M. Cheneau, D. Boiron, and C. I. Westbrook, Nature (London) **520**, 66 (2015).
[8] B. Chen, C. Qiu, S. Chen, J. Guo, L. Q. Chen, Z. Y. Ou, and W. Zhang, Phys. Rev. Lett. **115**, 043602 (2015).
[9] C. Qiu, S. Chen, L. Q. Chen, B. Chen, J. Guo, Z. Y. Ou, and W. Zhang, Optica **3**, 775 (2016).
[10] G. Campbell, M. Hosseini, B. M. Sparkes, P. K. Lam, and B. C. Buchler, New J. Phys. **14**, 033022 (2012).
[11] M. G. Raymer, I. A. Walmsley, J. Mostowski, and B. Sobolewska, Phys. Rev. A **32**, 332 (1985).
[12] L. M. Duan, M. D. Lukin, J. I. Cirac, and P. Zoller, Nature (London) **414**, 413 (2001).
[13] D. F. Phillips, A. Fleischhauer, A. Mair, R. L. Walsworth, and M. D. Lukin, Phys. Rev. Lett. **86**, 783 (2001).
[14] C. Liu, Z. Dutton, C. H. Behroozi, and L. V. Hau, Nature (London) **409**, 490 (2001).
[15] S. E. Harris, J. E. Field, and A. Imamoglu, Phys. Rev. Lett. **64**, 1107 (1990); S. E. Harris and Y. Yamamoto, *ibid.* **81**, 3611 (1998); S. E. Harris and L. V. Hau, *ibid.* **82**, 4611 (1999).
[16] M. Fleischhauer and M. D. Lukin, Phys. Rev. Lett. **84**, 5094 (2000).
[17] M. Fleischhauer and M. D. Lukin, Phys. Rev. A **65**, 022314 (2002).
[18] D. N. Matsukevich and A. Kuzmich, Science **306**, 663 (2004).
[19] I. Novikova, A. V. Gorshkov, D. F. Phillips, A. S. Sorensen, M. D. Lukin, and R. L. Walsworth, Phys. Rev. Lett. **98**, 243602 (2007).
[20] S. Zhou, S. Zhang, C. Liu, J. F. Chen, J. Wen, M. M. T. Loy, G. K. L. Wong, and S. Du, Opt. Express **20**, 24124 (2012).
[21] M. Fleischhauer, A. Imamoglu, and J. P. Marangos, Rev. Mod. Phys. **77**, 633 (2005).

[22] Y.-H. Chen, M.-J. Lee, I.-C. Wang, S. Du, Y.-F. Chen, Y.-C. Chen, and I. A. Yu, Phys. Rev. Lett. **110**, 083601 (2013).

[23] Y.-F. Hsiao, P.-J. Tsai, H.-S. Chen, S.-X. Lin, C.-C. Hung, C.-H. Lee, Y.-H. Chen, Y.-F. Chen, I. A. Yu, and Y.-C. Chen, Phys. Rev. Lett. **120**, 183602 (2018).

[24] J. Zhang, Z.-J. Gu, P. Qian, Z.-G. Han, and J.-F. Chen, Chin. Phys. Lett. **32**, 064211 (2015).

[25] K. F. Reim, J. Nunn, X.-M. Jin, P. S. Michelberger, T. F. M. Champion, D. G. England, K. C. Lee, W. S. Kolthammer, N. K. Langford, and I. A. Walmsley, Phys. Rev. Lett. **108**, 263602 (2012).